Research article

Jianfan Yang, Tian Qin, Fangxing Zhang, Xianfeng Chen, Xiaoshun Jiang and Wenjie Wan*

Multiphysical sensing of light, sound and microwave in a microcavity Brillouin laser

https://doi.org/10.1515/nanoph-2020-0176
Received March 7, 2020; accepted May 12, 2020

Abstract: Light, sound, and microwave are important tools for many interdisciplinary applications in a multiphysical environment, and they usually are inefficient to be detected simultaneously in the same physical platform. However, at the microscopic scale, these waves can unexpectedly interact with the same microstructure through resonant enhancement, making it a unique hybrid microsystem for new applications across multiple physical channels. Here we experimentally demonstrate an optomechanical microdevice based on Brillouin lasing operation in an optical microcavity as a sensitive unit to sense external light, sound, and microwave signals in the same platform. These waves can induce modulations to the microcavity Brillouin laser (MBL) in a resonance-enhanced manner through either the pressure forces including radiation pressure force or thermal absorption, allowing several novel applications such as broadband non-photovoltaic detection of light, sound-light wave mixing, and deep-subwavelength microwave imaging. These results pave the way towards on-chip integrable optomechanical solutions for sensing, free-space secure communication, and microwave imaging.

Keywords: microcavity; multiphysical sensing; optomechanics.

1 Introduction

Sensors, like eyes and ears of human beings, are the most important sensing units to respond to events in the environment, which is highly complex across multi-physical domains including signals from light, sound, electromagnetic waves, thermal, magnetic fields as well as electrical fields, etc. Previously, sensors can only operate in one particular physical field for the optimized performances and the sole response of materials. For example, a photodiode can hardly pick up any acoustic wave signals. Recent emerging developments in remote sensing [1], biomedical photoacoustic imaging [2], dual-band radio and optical communications [3] pose strong demands to implement hybrid multiphysical and compact devices for simultaneously sensing multiple waves/fields across different physical regimes. So far, such a hybrid sensor has not been demonstrated due to the rigid multiphysical responses required by materials. On the other hand, optomechanics, highly hybrid micro-devices, might just be the solution to the above problem. Previously, optomechanical devices have proved their ultrasensitive capability in mass sensing [4], force measurement [5], gas detection [6], as well as motion sensing [7, 8]. They can even be embedded in liquid environments for viscosity measurement [9] and particle sensing [10]. Particularly, incoming light can exert the radiation pressure force to these micro-devices and excite their optomechanical motions [11, 12]. Similarly, traditional acoustic fields can also induce modulations to these structures for sensing purposes [13]. However, it is not so trivial for microwave fields. It has been demonstrated that coherent coupling between microwaves and optical photons can be assisted by the radiation pressure, though, in vacuum conditions [14]. It is highly deserved to merge hybrid coupling of

***Corresponding author: Wenjie Wan**, The State Key Laboratory of Advanced Optical Communication Systems and Networks, University of Michigan-Shanghai Jiao Tong University Joint Institute, Shanghai Jiao Tong University, Shanghai, 200240, China; and MOE Key Laboratory for Laser Plasmas and Collaborative Innovation Center of IFSA, Department of Physics and Astronomy, Shanghai Jiao Tong University, Shanghai, 200240, China,
E-mail: wenjie.wan@sjtu.edu.cn. https://orcid.org/0000-0002-9743-3480
Jianfan Yang, Tian Qin and Fangxing Zhang: The State Key Laboratory of Advanced Optical Communication Systems and Networks, University of Michigan-Shanghai Jiao Tong University Joint Institute, Shanghai Jiao Tong University, Shanghai, 200240, China. https://orcid.org/0000-0002-8857-4919 (J. Yang)
Xianfeng Chen: MOE Key Laboratory for Laser Plasmas and Collaborative Innovation Center of IFSA, Department of Physics and Astronomy, Shanghai Jiao Tong University, Shanghai, 200240, China
Xiaoshun Jiang: National Laboratory of Solid State Microstructures and College of Engineering and Applied Sciences, Nanjing University, Nanjing, 210093, China

light, sound, and microwave in the same device for new functionalities, for example, in piezo-optomechanical circuits [15, 16].

Among many optomechanical platforms, microcavity Brillouin lasers (MBLs) can be fabricated in a compact form based on whispering-gallery resonances [17–19], where both optical waves and acoustic waves can be circularly and resonantly trapped to preserve high optical as well as mechanical Q factors. This greatly reduces lasing threshold [18, 20], permits ultra-narrow linewidth [21], which makes these micro-devices extremely sensitive to their surrounding medium for ultra-sensitive detection in massing sensing [4] as well as for others like force [5], gas [6], viscosity [9], and nanoparticle [10]. Moreover, the ultra-narrow linewidth feature and compactness of such MBLs can empower new types of inertial sensing applications as chip-scale optical gyroscopes [7]. Unlike traditional types of lasers sealed to work in a low-pressure condition, MBLs can be designed to operate in the ambient environment, which creates an ideal micro-platform for simultaneously sensing of multiphysical waves in an ambient environment. Such optomechanical nature and compact form factors pave the way for such devices' sensitive applications in sensing, remote control, and imaging.

In the work, we explore an optical-microcavity-based compact Brillouin laser system as an optomechanical probe to sense those induced modulation signals from external light, sound, and microwave sources in the same platform. We firstly demonstrate a microcavity Brillouin laser (MBL) based on a tapered-fiber-coupled microsphere assisted by its mechanical cantilever microstructure, which allows sensing the presence of the tiny radiation pressure force exerted from the external light, altering the lasing spectrum by precise optical actuation. Such a response can be resonantly enhanced through several mechanical resonances when temporal modulation is applied for both optical and acoustic fields. We validate the origins of these mechanical resonances by tuning their natural resonances through moving a load on the cantilever, effectively playing a micro-guitar string by the light. In the meantime, our MBL can simultaneously pick up these pressure waves from both light and sound, and coherently mix them into optical signals, opening up a unique gate for the dual-physical-channel communication. Additionally, the MBL can also react to the external microwave through material absorption. Based on that, we demonstrate a deep-sub-wavelength probe for microwave imaging. These results prove the MBL as a compact versatile tool in hybrid micro-systems for information processing, sensing, and imaging applications.

2 Results

2.1 A microcavity Brillouin laser

A Brillouin laser, a unique platform stimulating photons from coherent phonons, has found its crucial applications in optical inertial rotation sensing [22], microwave generation [23], and ultrafast amplitude modulation [24], thanks to its special features of narrow linewidth, broadband response, and less-material demand. The first demonstration of a Brillouin laser was in an optical-fiber ring resonator [25]. With recent developments in micro-fabrication and nanotechnology, more types of Brillouin lasers have emerged in a compact form such as MBLs [17, 18]. Like optical-electrostriction-induced stimulated Brillouin scattering in optical fibers [26, 27], both backward and forward types of Brillouin lasers can be found in these optical microcavities [28]. However, unlike in the fiber case, the resonant light field inside the microcavity can also induce optomechanical vibrations such as breathing modes through resonance-enhanced radiation pressure [29]. Careful engineering these mechanical structures can further permit phonon lasers [30]. Such hybrid micro-systems, with the coherent interplay between photons and phonons due to their optomechanical nature, can lead to many scientific advances and practical sensitive sensing applications.

Here our MBL is realized on a tapered-fiber-coupled microsphere resonator with $Q_{optical} > 10^8$ in the ambient environment. Such a microsphere made of a fused-silica fiber tip can support both optical and acoustic whispering-gallery type resonances (Figure 1a) where an optical pump light launched through the input port of the tapered fiber coincides with one optical whispering gallery mode (WGM) stimulating the generation of both a Stokes photon and an acoustic phonon through an electrostrictive-induced stimulated Brillouin scattering (SBS) process [28]. This SBS gain enables the observation of the MBL in our system. Unlike previous Brillouin Lasers from the backward SBS [18], our MBL is from the forward SBS (verified by a Fabry–Perot cavity measurement in the supplementary notes), resulting in a Stokes shift around 66.9 MHz. This MBL, established from the Doppler-shifted pump light, hits another optical WGM fulfilling the phase-matching condition as shown in Figure 1b. In the meantime, the excited phonon also hits the acoustic WGM (Figure 1a bottom) which strongly enhances the internal acoustic field. On one hand, this triple-resonant configuration (i. e., the pump photon, the Stokes photon, and the acoustic phonon) allows us to observe the MBL at a very low pumping threshold, as low as 1.25 mW with a steep pump-output

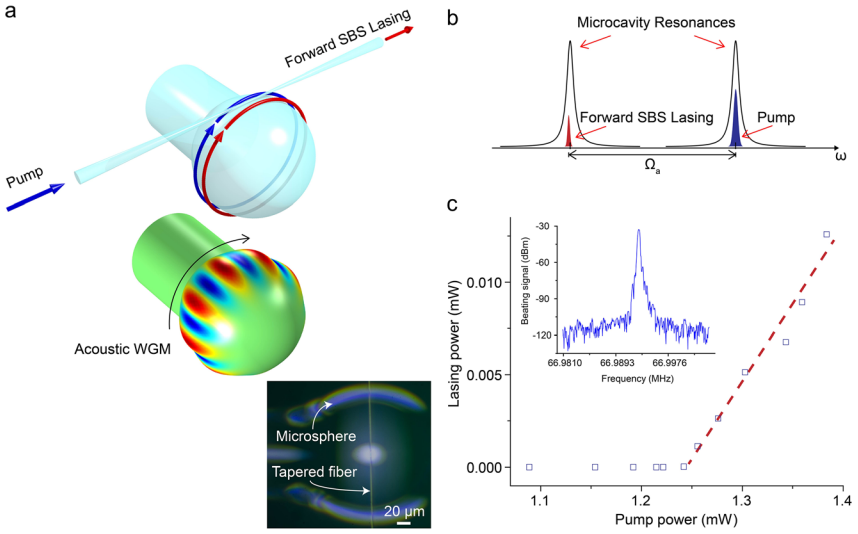

Figure 1: Conceptual illustration of a microcavity Brillouin laser (MBL). (a) A forward SBS laser in a microsphere. Top: a pump light guided by a tapered fiber is evanescently coupled into one of the optical WGMs of a microsphere and induces forward SBS lasing which also resonantly propagates in another optical WGM. This signal light is evanescently coupled back to the same tapered fiber. Bottom: a Rayleigh-type surface acoustic wave unidirectionally propagates in an acoustic WGM. Inset: a photo of the microsphere coupling system. Scale bar: 20 μm (b) Spectrum diagram of an MBL in a resonance-enhanced system. The pump light (blue) is at the center of an optical WGM. The forward SBS lasing signal (red) is near the center of another optical WGM. The frequency difference between the pump and the signal is the frequency of the electrostriction-induced acoustic wave. (c) Pump power versus forward SBS lasing power curve. The slope efficiency is 0.1. Inset: The optical beating between the pump light and the lasing signal obtained from the electrical spectrum analyzer. The blue squares are the experimental data and the red dashed line is from the linear fitting.

slope as shown in Figure 1c, where tiny changes may be reflected in the output power. On the other hand, the rigid phase-matching condition in this triple-resonant system can be easily disturbed by thermal, mechanical, or vibrational noises from its surroundings, making it a good platform for sensitive-detection applications [6, 31]. In our experimental set-up, both the microsphere and the tapered fiber are physically extended from a standard silica fiber which is very flexible, only 125 μm in diameter; moreover, our MBL operates near the lasing threshold where even a tiny external noise may greatly influence this opto-mechanical system. In the following, we will experimentally explore the external light, sound, and microwave sources' impact on this MBL.

2.2 Radiation pressure induced actuation in MBL

Firstly, we demonstrate the light-induced radiation pressure sensing capability in our MBL by sensitive detecting induced actuation (Figure 2). It is well-known that light can induce the radiation pressure force to matter due to the conserved photon momentum [29]. However, given the

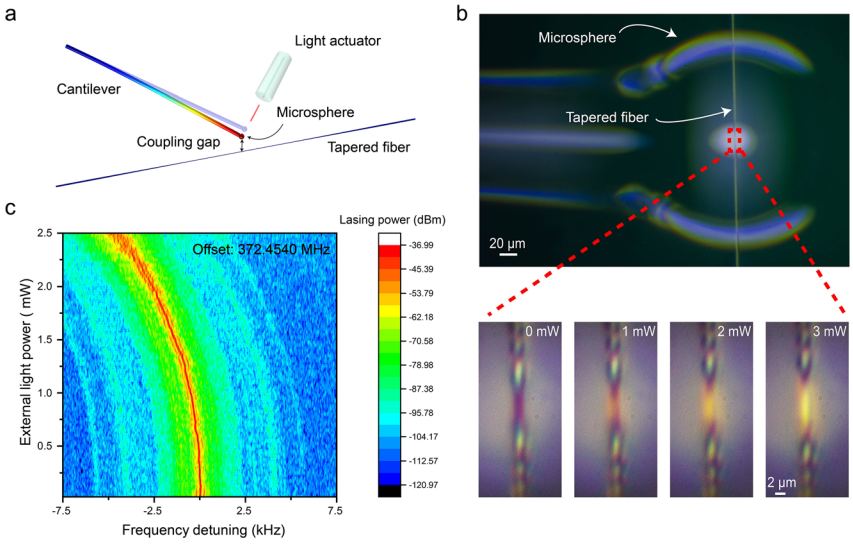

Figure 2: Tuning MBL by optical radiation pressure. (a) Schematic illustration of the gap-spacing changing between the microsphere and the tapered fiber by a CW laser beam shooting at the microsphere. The coupling gap is around 200 nm. The distance between the light actuator and microsphere is 10 μm. The spot size on the microsphere is around 10 μm. (b) Direct gap-spacing observation through Newtown's ring pattern. (c) Evolution diagram of the MBL frequency shift induced by optical actuation. The lasing offset frequency is around 372.4540 MHz.

limited power of light sources, such radiation pressure force is usually weak, only felt by microscopic objects, for example, optical trapping nano/micro-particles [32]. Here our MBL is a "mesoscopic" one consisting of a microscopic microsphere resonator (around 175 μm in diameter) and a macroscopic long pillar (over 6.2 mm in length). Both of these features can affect the generation of the MBL in our experiment. When the MBL is turned on, we shine an external fiber-coupled laser to the microsphere to investigate such effect as shown in Figure 2a. The main radiation pressure force (numerically estimated as 1.61 pN for 1.00 mW inputs, see the supplementary notes) performs as an optical actuator pushing the microsphere at the end of the cantilever pillar away from its mean position (Figure 2b). Noticeable variation can be observed in Newton's ring pattern arising from the interference between the tapered fiber and the microsphere in the evanescent coupling region, which clearly implies the gap-spacing changing due to this external radiation pressure force.

Alternatively, we calibrate such gap changing with a separated experiment using a nanometer-resolution piezoelectric actuator and find out the actuation to be around 150 nm for an equivalent 3 mW laser-induced shift. As a result, the MBL is red-shifted around 5 kHz spectrally, giving a resolution of 1 kHz which is the linewidth of the MBL (supplement). A similar relationship between the MBL threshold and the coupling efficiency has been studied previously in Ref [28]. These behaviors origin from the gap changing in the evanescent coupling region causing the small detuning of WGM resonances [33], which are precisely aligned according to the phase-matching conditions for both the pump and the Stokes lasers. Moreover, similar phenomena can be observed with 633, 1064, and 1550 nm external laser for the optical actuation (results for 633 nm and 1550 nm are shown in the supplement). Intuitively, this arises from radiation pressure from any light despite its frequency. This sensing scheme effectively offers an alternative non-photovoltaic solution to the sensitive light-field detection through the radiation pressure force, which should respond in a broadband manner other than the material-limited bandwidth in photovoltaic detection.

2.3 Optical modulation of MBL and micro-guitar demonstration

More insights can be gained by performing a dynamical modulation to our cantilever-microcavity optomechanical system as shown in Figure 3a. The external laser source is temporally modulated while maintaining its power level. By sweeping the modulation frequency, two resonances appear at 2.384 and 15.169 kHz (Figure 3c) by reading out the MBL's variation signal through a lock-in detection scheme (method). These resonances are the mechanical responses from the cantilever pillar excited by the radiation pressure force, similar to previous works using the AFM cantilever [34]. Numerically, we verify these two mechanical modes to

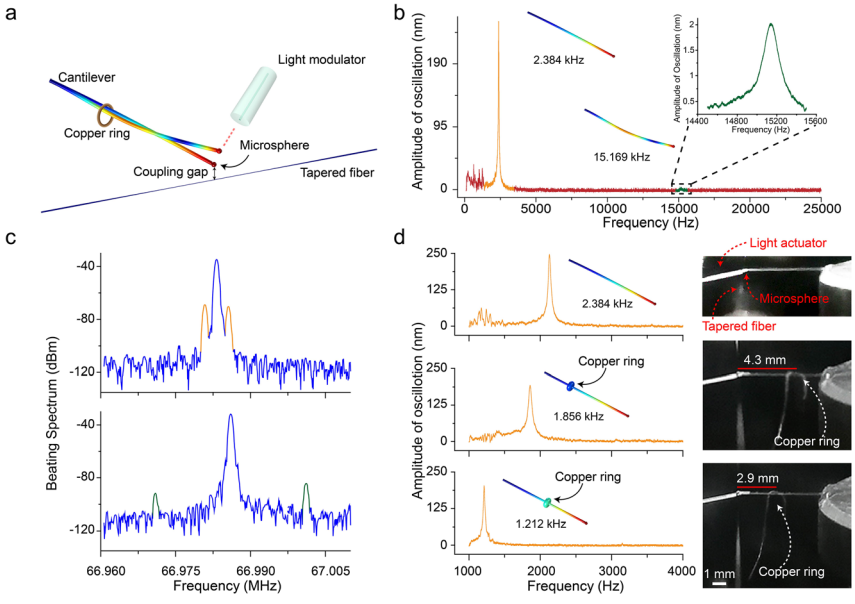

Figure 3: MBL optical induced modulation. (a) Schematic illustration of different mechanical modes of the cantilever-microsphere structure excited by a modulated laser beam shooting at the microsphere. Coupling gap: around 200 nm. Distance between light actuator and microsphere: 10 μm. Spot size: 10 μm. Cantilever length: 6.2 mm. (b) Oscillation spectrum of two different mechanical modes from the cantilever-microsphere structure. The optical modulation depth is less than 500 μW. Different mechanical motions via FEM are shown. Inset: diagram of the mode at 15.169 kHz in detail. (c) Spectrum of MBL under optical modulation obtained from the electrical spectrum analyzer. (d) Micro-guitar demonstration. The fundamental mechanical mode of the cantilever-microsphere structure is red-shifted when a copper ring is getting closer to the microsphere. Different mechanical motions of a donut-shaped loading via FEM are shown. The loading position from top to bottom: loading-free; 4.3 mm away from the microsphere; 2.9 mm away from the microsphere. The scale bar: 1 mm.

be 2.392 and 15.000 kHz respectively by simulating the cantilever-microsphere structure via FEM.

Such mechanical oscillations sinusoidally modulate the MBL exhibiting two beating sidebands in the spectrum domain (Figure 3d). This effectively constructs an optical receiver for free-space communication, which is, as mentioned above, non-photovoltaic and applicable for almost all wavelengths as long as the radiation pressure is present. Ideally, our system can reach a sensitivity to read out even the Brownian motion of the coupling tapered fiber [8, 35], but improvements to the system stability and detection scheme have to be considered for further studies. In the experiment, we estimate the optical sensitivity at the modulation frequency of 2.384 kHz. The modulated optical beam applies a driving force at this natural frequency and greatly amplifies the mechanical motion. Compared with the continuous-wave actuation, the enhancement factor is around 20 according to the quality factor of the mechanical oscillation. Meanwhile, the phase-sensitive lock-in detection method further improves the signal-to-noise ratio. Practically, we realize the minimum optical radiation pressure force of $2\text{fN} \cdot \text{Hz}^{-1/2}$ with the minimum optical power fluctuation of 100 nW, which is 1000 times greater than the sensitivity in the continuous-actuation case (supplement). Moreover, we can tune the natural frequencies of the cantilever-microsphere structure by either increasing or redistributing the weight on the pillar, effectively optically playing a "micro-guitar". In our experiment, a thin copper ring is suspended on and oscillates with the pillar. As shown in Figure 3d, by loading and moving the thin copper ring towards the microsphere side, the resonance can be tuned from the original 2.384 kHz (unloaded) to 1.856 kHz (loaded at 4.3 mm away from the microsphere), and finally reaching 1.212 kHz (loaded at 2.9 mm away from the microsphere), respectively. Meanwhile, a model of a pillar with a donut-shaped load carrying similar weight at different positions is established via FEM and this oscillation simulation coincides well with the experimental results shown in Figure 3d inset. This is an important result. On one hand, such cantilever resonances can directly amplify weak modulation signals at some specific frequency for enhanced sensitivity. On the other hand, with the help of such a tuning mechanism, one can select the interested frequency band to amplify. Moreover, it opens up a new optomechanical way for sensitive mass-sensing applications [4].

2.4 Acoustic wave sensing in MBL

Inspired by the above optical modulation experiment, we also investigate an acoustic way to modulate our MBL by directly shining an acoustic wave from a micro-speaker as shown in Figure 4a. This acoustic wave provides the

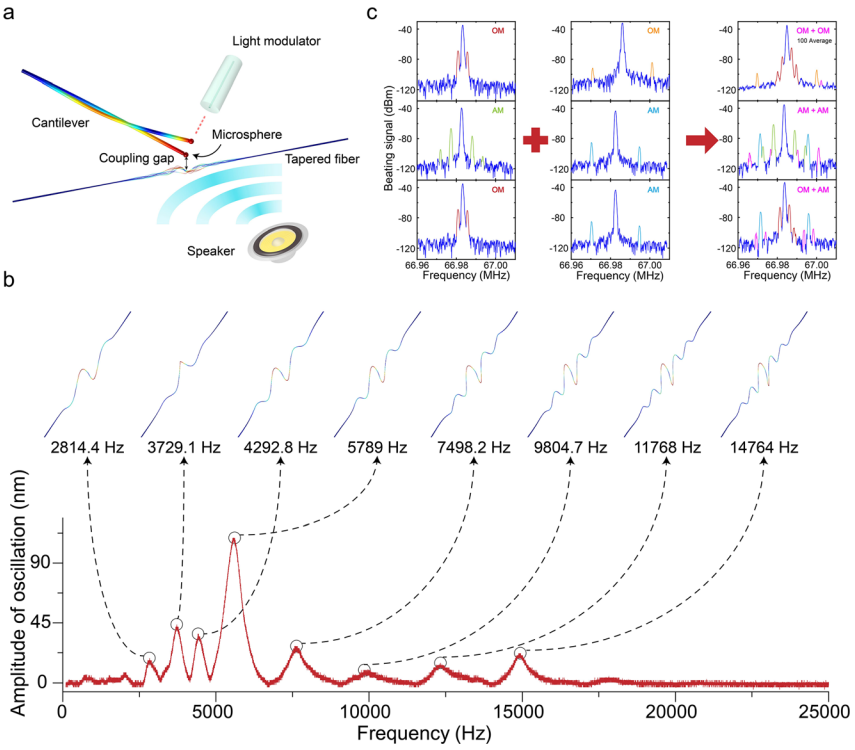

Figure 4: MBL acoustic induced modulation and hybrid dual-channel communications. (a) Schematic illustration of the mechanical modes of the cantilever-microsphere structure and the tapered fiber excited by a temporally-modulated laser beam and a sound wave, respectively. Coupling gap: around 200 nm. Distance between light actuator and microsphere: 10 μm. Spot size: 10 μm. Distance between speaker and tapered fiber: 15 mm. Cantilever length: 6.2 mm. Tapered fiber length: 52 mm. (b) Oscillation spectrum of different mechanical modes from the tapered fiber "string". Each mode has been verified by FEM (inset). (c) Demonstration of the dual-channel communications. Each row represents a combination of waves acting on the MBL. OM: optical modulation. AM: acoustic modulation. The magenta color represents the generating frequency.

driving force from the air and fluctuates the MBL structure to realize the acoustic modulation. Considering the flicker noise, one of the dominant noises in the acoustic frequency domain, our system converts this acoustic signal out of the low-frequency band optically to get rid of the flicker noise. In the experiment, the tapered fiber is suspended on a D-shape holder. Only the two ends of the tapered fiber are stuck through UV glue, and the distance between these two ends is viewed as the total length to oscillate. The tapered fiber is slightly tightened up to stable the MBL and avoid intensive stress. By beating with MBL's native resonance, we can coherently pick up those acoustical signals in a more sensitive way with sensitivity ~267 μPa $Hz^{-1/2}$ (details in the supplement), comparable or better performed than other similar optomechanical devices [36]. Here multiple resonances are observed from the MBL's spectrum response during frequency sweeping in Figure 4b. However, these modes are relatively broad with lower mechanical Q factor (~5) as compared to those in the optical case (mechanical Q factor ~50). This is because the acoustic field is much wider than the laser field which is more directional and purposely pointed only to the microsphere resonator. As a result, the tapered fiber with nearly 5 cm length reacts much stronger to this sound wave due to its micrometer-size width which makes it flexible to flow even in the air. The greater damping effect arising from the surrounding airflow degrades its mechanical Q. We numerically examine these oscillation modes from such fiber "strings" and find each one's corresponding resonance as shown in Figure 4b. Similar results have also been demonstrated in a vacuum environment but with a higher Q factor [8, 35]. In order to distinguish sensed signals from light or sound, we note that these resonance peaks are quite distinct in the frequency domain. For example, only two resonances with much higher Q factors exhibit for the optical sensing as compared to eight lower Q resonant modes in the acoustic case. This feature can be utilized for separating out sensed signals. Moreover, the optically induced resonances are tunable as mentioned above in the micro-guitar experiment, which can be further developed for the signal decoupling purpose.

Another major feature utilizing this new acoustic tool, we proceed to demonstrate an interesting dual physical channel mixing through both optical and acoustic physical channels shown in Figure 4c. Three types of combinations: optical-optical, acoustic-acoustic, and optical-acoustic dual-channel communications are explored, where their frequency mixing can be clearly illustrated in the MBL's beating spectrum (Figure 4c). This is achieved by sending signals through light and sound simultaneously at those resonance modes mentioned above, and those off-resonance signals either through light or sound are less pronounced. Further, potential cross modulation is carefully minimized by positioning the light modulator and the speaker shown in Figure 4a. Specifically, the inclined light incidence keeps the light spot away from the tapered fiber. In the meantime, although the pillar is inevitably and always covered with the spreading sound wave, horizontally positioning the speaker greatly eliminates the pressure force which fluctuates the pillar in the vertical direction and further suppresses cross modulation (supplement). Here for the three kinds of mode mixings, they all can be understood as temporal modulations exerted from these external waves simultaneously, where both optical and acoustic waves can induce resonant oscillation to the cantilever and the tapered fiber, respectively, through the sensitive fiber evanescent coupling scheme. On the other hand, those mixed resonances (highlighted in pink) naturally act as AND gates, where only if both input channels are present, their sum-frequency signals can be picked up. Based on this property, the MBL system acts as the decryption tool to reveal the information which is encoded from two physical channels like light and sound. Only if both physical signals are detected simultaneously via the MBL system, the encrypted information can be revealed, providing a new way towards free-space secure communication. Lastly, identical pairs of MBLs are obtainable to improve bit error rate and relay the signals. Physical channel calibration can be realized by adjusting the loading position on the cantilever and gluing part of the taper-free regions of the tapered fiber (supplement). Previously coupling acoustic and optical signals together relies on the piezoelectric material [15, 16]. Light modulation from free space often requires a low-pressure environment which inherently limits the possibility of introducing the sound wave [34]. Unlike these prior works, the sensitive MBL system releases the vacuum condition and embraces the pressure waves from the ambient environment, also possible in a liquid environment [13], making it more accessible for sensing and free-space communication applications [37].

2.5 MBL microwave sensing and deep-subwavelength microwave imaging

At last, we investigate another common electromagnetic wave, i. e., microwave's influence on the MBL system. The MBL is placed nearby a dipole antenna of an external microwave source (Figure 5a), which is swept continuously in frequency and gradually pumped up the power level to probe the response of the MBL. As a result, the MBL's central frequency red-shifts up to 20 kHz when increasing the power

of the microwave source to 40 mW (Figure 5b). In principle, this frequency shifting will not influence the functionality of the light/sound sensing since the modulated sideband will be shifted along with the center frequency (supplement). Now, MBL central frequency tuning, viewed as the signature of the microwave sensing, potentially completes the last puzzle to realize simultaneously sensing light, sound, and microwave. According to the slope of the MBL shifting, the steepest slope is 2.9029 kHz/mW (supplement). Experimentally the pump light can act as another heat source to tune the temperature around the microsphere, which adds another degree of freedom to set the MBL in different phase-matching conditions. In this way, we can constantly make use of the steepest slope to improve sensitivity. At microwave frequency of 7.5 GHz, we have realized the minimum microwave power detection of 0.3 mW which highly depends on whether the MBL is under the rigid phase-matching conditions. In the meantime, several resonances are observed in the response of the MBL's intensity in the frequency span from 4.7 to 12.0 GHz during a constant-power frequency sweeping where a more broadband response is expected to be revealed in further studies (Figure 5c). Unlike the previous modulation schemes through pressure waves, we contribute these behaviors to

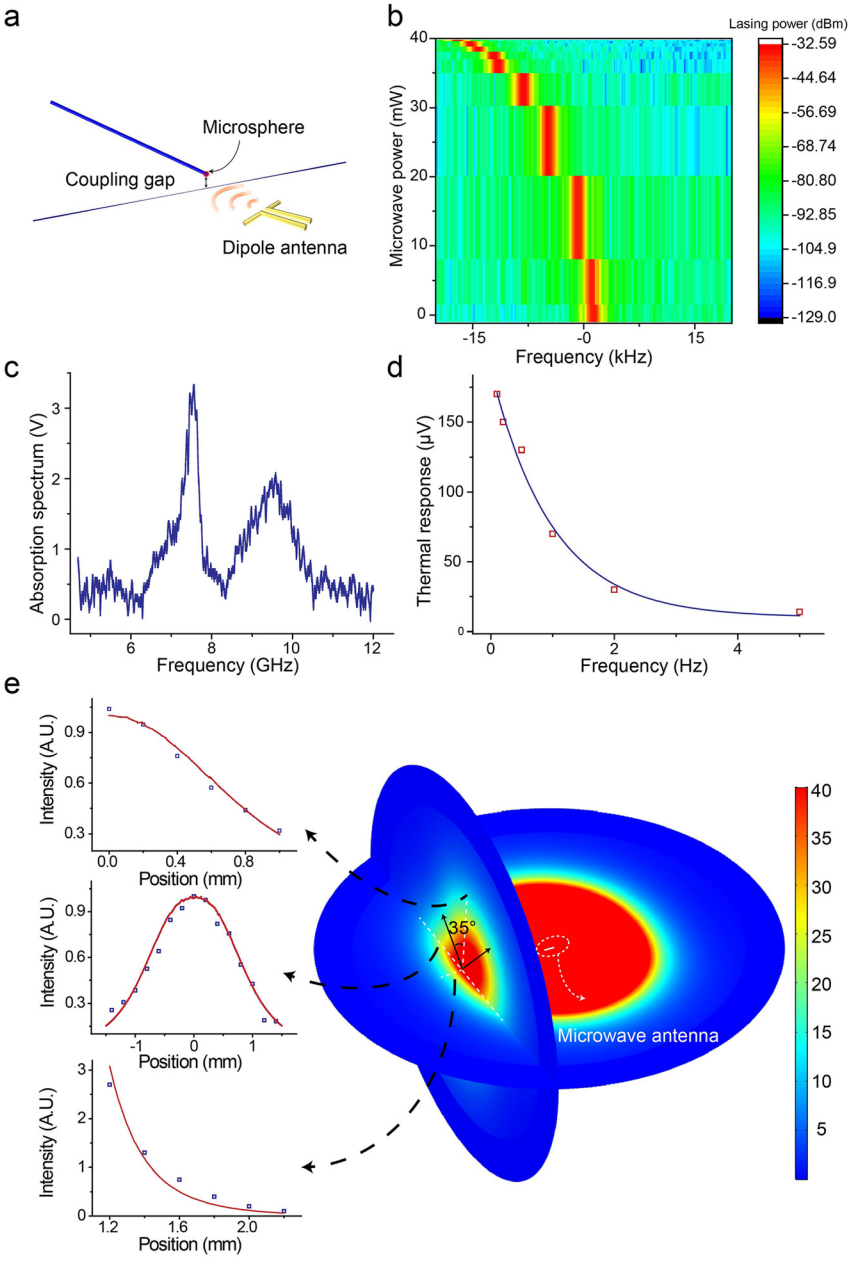

Figure 5: MBL microwave-induced modulation and subwavelength profile scanning.
(a) Schematic illustration of a microsphere experiencing thermal effects excited by a microwave. Coupling gap: contact with tapered fiber (also workable within 200 nm). Distance between dipole antenna and microsphere: 1.2 mm. (b) Evolution diagram of the MBL frequency shift induced by the microwave modulation. The lasing offset frequency is around 469 MHz. The microwave frequency is at 7.5 GHz. (c) Absorption spectrum of a microsphere heated by microwave. (d) Thermal response of the MBL by a modulated microwave. The microwave frequency is at 7.5 GHz. The red squares are the experimental data and the blue curve is from the exponential fitting. (e) Demonstration of 3D microwave profile scanning. Right: FEM simulation of a microwave profile from a microwave antenna. The orientation of the dipole antenna is shown. The angle between the antenna plane and the vertical scanning axis is around 35°. Left: vertical, horizontal, and longitudinal microwave power distribution from top to bottom, respectively. The red lines are from FEM simulation and the blue squares are from experimental data.

the thermal effects caused by the material absorption. Here the silica microsphere is well-known for being covered with a thin water layer in the ambient environment [38]. This layer strongly absorbs the microwave radiation in the spectrum of several GHz frequencies [39]. Moreover, prior studies also suggest some resonant peaks in the silica's absorption spectrum we're interested in here [40]. In either way, such material absorption can lead to the microcavity's internal temperature rising, causing the resonances red-shifting through a thermal-optical effect [41]. We verify the above proposed theory by performing a temporal modulation experiment and observe a characteristic exponential decay response of the MBL when ringing up the modulation frequency from 100 mHz to 5 Hz (Figure 5d), which indicates a slow thermal effect through heat conduction between the absorption regime and the optical-mode regime, similar with the prior studies [42]. Moreover, additional tests are conducted by adjusting the microwave's power to observe the red-shifting of optical modes in our microcavity. These results verify the thermal-optical nature of the MBL by heating through a microwave source, much similar to our previous work of heating microcavity through light [43]. With the help of a numerical tool to simulate the temperature distribution through heat conduction, we can calculate the slope efficiency of the temperature variation versus the input microwave power as 5.23 mK/mW (supplement). Such techniques can be applied for precise frequency-tuning in a microcavity, which is very crucial for microcavity based applications since the tuning methods are limited at this microscale. Prior works using mechanical pulling/compression through photo-elastic effect has been realized in hollow bottle-like microresonators (BLMR) [44], while its tuning resolution proportional to the mechanical stretching is limited by mechanics. Here microwave heating in our MBL system offers another approach for fine-tuning in a remote manner, which may be applicable even in vacuum conditions.

We explore this MBL's unique response to the microwave as a feasible tool for a deep-subwavelength microwave imaging application. As a proof-of-principle experiment, we perform a profile scanning near a microwave antenna as shown in Figure 5e. In the experiment we change the position of the dipole antenna in three dimensions to let the MBL experience different parts of the microwave field. Here the working frequency of the emitted microwave is fixed at 7.5 GHz, i. e., ~ 4.0 cm in wavelength. The microwave receiver based on a silica microsphere only has a radius of 85 μm, ~1/250 of the wavelength. Such a deep-subwavelength microwave sensor may be beneficial for some critical experiments in the condensed matter [45], quantum physics [46], and metrology [47]. In principle, the form factor can be further reduced if implementing these optomechanical processes on a chip [29]. After scanning, the obtained MBL power response can resemble the near-field microwave profile; as compared to the numerically calculated emission pattern near an antenna, our method accurately maps out this field distribution in all three dimensions. Currently our MBL records total power in all polarizations. A polarization-sensitive MBL requires either asymmetric structure such as microdisk or anisotropic material for material absorption such as a one-directional nanowire array, which is worth further investigation. We believe this new technique can bring a new tool for applications in microwave imaging and spectroscopy.

3 Discussion

In summary, we experimentally demonstrate a compact optomechanical system based on a MBL, which can sense induced modulation from external light, sound and microwave sources through the cantilever-microsphere structure, the tapered fiber motion and the microwave absorption, respectively, in the same microstructure. These independent degrees of freedom naturally distribute signals to different channels in a distinguishable manner, offering us an opportunity to implement such a hybrid sensing micro-platform for new applications. Such a hybrid sensing ability of our hybrid micro-system can lead to new revolutionary technologies in many areas. For example, we have shown acoustic and optical induced mixing in the MBL, which has the potential in sound-light dual physical channel communications. This allows information to travel separately through two physical channels, i. e., optical one (information) and acoustical one (security key), and finally combine in the same MBL sensor. By doing this, we can hide encrypted information on either channel for security purposes [48]. Moreover, we have also shown the tunability of the cantilever resonances by shifting the small weight in our MBL. Note that these resonances can also fit into the operation spectrum of the underwater sonar system [49], providing a compact and sensitive solution for underwater navigation and communication purposes. At last, our demonstration of the deep-subwavelength microwave field scanner by the MBL is another alternative way for broadband microwave sensing with optics, which can operate in the ambient environment without the extra effort for either special materials or vacuum isolation, making it feasible for microwave related applications. In the future, we expect to merge the three sensing capability into one integrated platform by optimizing the corresponding microstructures

as well as the microsphere material, i. e., for fast-response microwave sensing, such that the interplay of the three sensing channels will further enable new functionalities. We believe this new hybrid micro-device will open up new possibilities in many areas including but not limited to information processing, sensing, and imaging applications.

4 Materials and methods

Cantilever-microsphere fabrication. A standard single-mode fiber (G.652.D) without cladding is fused by an electric arc from a fiber fusion splicer (Ericsson FSU 995 FA) in the ambient environment. A complete fusion process makes a microsphere with a radius of 85 μm. We stick this piece of fiber on a heavy post with UV glue and make sure the length of the cantilever is around 6 mm.

Tapered-fiber fabrication. A standard single-mode fiber (G.652.D) without cladding is softened by a hydrogen lamp and is slowly tapered in both directions at the same speed. A real-time observation of the light transmission on the oscilloscope is required to adjust the flame and determine the shut-down moment. The tapered region is around 4.2 cm. The time cost during the taper process is within 15 min.

Wave emitters. Our light emitter is a standard single-mode fiber (G.652.D) with flat ends. No special collimator or micro-lens is added. Our sound emitter is a commercial headphone unit driven by a function generator (Siglent SDG5162). Our microwave emitter is a home-made dipole antenna. Two copper wires aligned with a gap smaller than 100 μm are connected with the anode and the cathode of an electric cable. The radius of each copper wire is around 50 μm.

Light tuning experiment. The pump light is from Toptica CTL and the wavelength is around 1557 nm. The external light is from Toptica DL Pro and the wavelength is around 1550 nm. A function generator (Siglent SDG5162) is used to do the modulation. This electric signal is divided into two channels and one of them is sent to the lock-in amplifier (SRS SR865A) as the reference signal. We use an EOM to modulate the external light beam. The modulation depth can be reduced to 500 nW, as long as the lock-in amplifier can detect the signal from the noise. In the light-light communication demonstration, two frequencies from two channels of the function generator are applied on the same EOM simultaneously.

Sound tuning experiment. The signal from the function generator is sent to the anode and the cathode of the headphone unit. A typical value of the signal is below 1 V. The distance between the acoustic modulator and the microsphere is around 1.5 cm. In the sound-sound communication demonstration, two frequencies from two channels of the function generator are applied on the anode and the cathode simultaneously.

Microwave tuning experiment. The microwave modulator is placed over 1.2 mm away from the microsphere to avoid disturbing the temperature of the surrounding air through thermal conductance which would cool the temperature of the microsphere unexpectedly. A microwave mixer (REMEC Magnum MC44P-12) is used to modulate the microwave signal. Specifically, LO channel is connected with the microwave generator (Agilent Technology E8257D), IF channel is connected with the function generator, and RF channel goes through the microwave amplifier (CTT ALN/079-2025-41) before reaching the microwave emitter. To obtain Figure 5c and Figure 5e, we generate a 1 Hz sinusoidal signal by the function generator and divide this signal into two channels, one to IF channel, the other to lock-in amplifier as the reference signal. The amplitude of the signal is 4 V, which will modulate the amplitude of the microwave over 20 dB. In both cases, the power of the microwave is set 18 dBm from the microwave generator. In the end, the MBL experiences a small disturbance at 1 Hz. Namely, the intensity of this disturbance expresses the MBL's response to the microwave. In our experiment, the frequency filter from the lock-in is set at 0.3 Hz, which requires the exposure of at least 10 s for one stable and convincing measurement. To plot Figure 5e, it takes within 15 min to finish all the measurements with adjusting stage.

Signal processing. To detect the MBL modulation from a lock-in amplifier, a square-law detector (AD8310) is used after the beating signal going through a photodetector. When modulation happens, the optical beating frequency Ω_a with its sidebands $\Omega_a + \Omega$ and $\Omega_a - \Omega$ goes through the square-law detector, and the envelope is extracted. This envelope, frequency at Ω, shows the modulation depth of the MBL on the lock-in amplifier.

Acknowledgments: This work was supported by National key research and development program (Grant No. 2016YFA0302500, 2017YFA0303700); National Science Foundation of China (Grant No. 11674228, No. 11304201, No. 61475100); Shanghai MEC Scientific Innovation Program (Grant No. E00075); Shanghai Scientific Innovation Program (Grant No. 14JC1402900); Shanghai Scientific Innovation Program for International Collaboration (Grant No. 15220721400).

Author contribution: All the authors have accepted responsibility for the entire content of this submitted manuscript and approved submission.

Research funding: None declared.

Employment or leadership: None declared.

Honorarium: None declared.

Conflict of interest statement: The authors declare no conflicts of interest regarding this article.

References

[1] J. G. P. W. Clevers and H. J. C. Van Leeuwen, "Combined use of optical and microwave remote sensing data for crop growth monitoring," *Remote. Sens. Environ.*, vol. 56, no. 1, pp. 42–51, 1996.

[2] M. Xu and L. V. Wang, "Photoacoustic imaging in biomedicine," *Rev. Sci. Instrum.*, vol. 77, no. 4, p. 041101, 2006.

[3] J. R. Bruzzi and B. G. Boone, "Dual band radio frequency (RF) and optical communications antenna and terminal design methodology and implementation," U.S. 8094081, 2012.

[4] F. Liu, S. Alaie, Z. C. Leseman, and M. Hossein-Zadeh, "Sub-pg mass sensing and measurement with an optomechanical oscillator," *Opt. Express*, vol. 21, no. 17, pp. 19555–19567, 2013.

[5] E. Gavartin, P. Verlot, and T. J. Kippenberg, "A hybrid on-chip optomechanical transducer for ultrasensitive force measurements," *Nat. Nanotech.*, vol. 7, no. 8, pp. 509–514, 2012.

[6] B. Yao, C. Yu, Y. Wu, et al., "Graphene-enhanced Brillouin optomechanical microresonator for ultrasensitive gas detection," *Nano Lett.*, vol. 17, no. 8, pp. 4996–5002, 2017.
[7] J. Li, M. G. Suh, and K. Vahala, "Microresonator brillouin gyroscope," *Optica*, vol. 4, no. 3, pp. 346–348, 2017.
[8] A. G. Krause, M. Winger, T. D. Blasius, Q. Lin, and O. Painter, "A high-resolution microchip optomechanical accelerometer," *Nat. Photon.*, vol. 6, no. 11, pp. 768–772, 2012.
[9] K. H. Kim, G. Bahl, W. Lee, et al., "Cavity optomechanics on a microfluidic resonator with water and viscous liquids," *Light Sci. Appl.*, vol. 2, no. 11, p. e110, 2013.
[10] W. Yu, W. C. Jiang, Q. Lin, and T. Lu, "Cavity optomechanical spring sensing of single molecules," *Nat. Commun.*, vol. 7, no. 1, p. 12311, 2016.
[11] H. Li, Y. Chen, J. Noh, S. Tadesse, and M. Li, "Multichannel cavity optomechanics for all-optical amplification of radio frequency signals," *Nat. Commun.*, vol. 3, no. 1, p. 1091, 2012.
[12] M. Li, W. H. P. Pernice, C. Xiong, T. Baehr-Jones, M. Hochberg, and H. X. Tang, "Harnessing optical forces in integrated photonic circuits," *Nature*, vol. 456, no. 7221, pp. 480–484, 2008.
[13] K. H. Kim, W. Luo, C. Zhang, et al., "Air-coupled ultrasound detection using capillary-based optical ring resonators," *Sci. Rep.*, vol. 7, no. 1, p. 109, 2017.
[14] R. W. Andrews, R. W. Peterson, T. P. Purdy, et al., "Bidirectional and efficient conversion between microwave and optical light," *Nat. Phys.*, vol. 10, no. 4, pp. 321–326, 2014.
[15] J. Bochmann, A. Vainsencher, D. D. Awschalom, and A. N. Cleland, "Nanomechanical coupling between microwave and optical photons," *Nat. Phys.*, vol. 9, no. 11, pp. 712–716, 2013.
[16] K. C. Balram, M. I. Davanço, J. D. Song, and K. Srinivasan, "Coherent coupling between radiofrequency, optical and acoustic waves in piezo-optomechanical circuits," *Nat. Photon.*, vol. 10, no. 5, pp. 346–352, 2016.
[17] I. S. Grudinin, A. B. Matsko, and L. Maleki, "Brillouin lasing with a CaF2 whispering gallery mode resonator," *Phys. Rev. Lett.*, vol. 102, no. 4, p. 043902, 2009.
[18] M. Tomes and T. Carmon, "Photonic micro-electromechanical systems vibrating at X-band (11-GHz) rates," *Phys. Rev. Lett.*, vol. 102, no. 11, p. 113601, 2009.
[19] K. J. Vahala, "Optical microcavities," *Nature*, vol. 424, no. 6950, pp. 839–846, 2003.
[20] N. Dostart, S. Kim, and G. Bahl, "Giant gain enhancement in surface-confined resonant Stimulated Brillouin Scattering," *Laser & Photon. Rev.*, vol. 9, no. 6, pp. 689–705, 2015.
[21] M. G. Suh, Q. F. Yang, and K. J. Vahala, "Phonon-limited-linewidth of Brillouin lasers at cryogenic temperatures," *Phys. Rev. Lett.*, vol. 119, no. 14, p. 143901, 2017.
[22] F. Zarinetchi, S. P. Smith, and S. Ezekiel, "Stimulated Brillouin fiber-optic laser gyroscope," *Opt. Lett.*, vol. 16, no. 4, pp. 229–231, 1991.
[23] X. S. Yao, "High-quality microwave signal generation by use of Brillouin scattering in optical fibers," *Opt. Lett.*, vol. 22, no. 17, pp. 1329–1331, 1997.
[24] S. P. Smith, F. Zarinetchi, and S. Ezekiel, "Narrow-linewidth stimulated Brillouin fiber laser and applications," *Opt. Lett.*, vol. 16, no. 6, pp. 393–395, 1991.
[25] K. O. Hill, B. S. Kawasaki, and D. C. Johnson, "CW Brillouin laser," *Appl. Phys. Lett.*, vol. 28, no. 10, pp. 608–609, 1976.
[26] E. P. Ippen and R. H. Stolen, "Stimulated Brillouin scattering in optical fibers," *Appl. Phys. Lett.*, vol. 21, no. 11, pp. 539–541, 1972.
[27] R. M. Shelby, M. D. Levenson, and P. W. Bayer, "Resolved forward Brillouin scattering in optical fibers," *Phys. Rev. Lett.*, vol. 54, no. 9, pp. 939–942, 1985.
[28] G. Bahl, J. Zehnpfennig, M. Tomes, and T. Carmon, "Stimulated optomechanical excitation of surface acoustic waves in a microdevice," *Nat. Commun.*, vol. 2, no. 1, p. 403, 2011.
[29] T. J. Kippenberg and K. J. Vahala, "Cavity optomechanics: back-action at the mesoscale," *Science*, vol. 321, no. 5893, pp. 1172–1176, 2008.
[30] I. S. Grudinin, H. Lee, O. Painter, and K. J. Vahala, "Phonon laser action in a tunable two-level system," *Phys. Rev. Lett.*, vol. 104, no. 8, p. 083901, 2010.
[31] G. Bahl, K. H. Kim, W. Lee, J. Liu, X. Fan, and T. Carmon, "Brillouin cavity optomechanics with microfluidic devices," *Nat. Commun.*, vol. 4, p. 1994, 2013.
[32] A. Ashkin, "Acceleration and trapping of particles by radiation pressure," *Phys. Rev. Lett.*, vol. 24, no. 4, p. 156, 1970.
[33] D. R. Rowland and J. D. Love, "Evanescent wave coupling of whispering gallery modes of a dielectric cylinder," *IEE Proc. J. (Optoelectronics)*, vol. 140, no. 3, pp. 177–188, 1993.
[34] D. Kleckner and D. Bouwmeester, "Sub-kelvin optical cooling of a micromechanical resonator," *Nature*, vol. 444, no. 7115, pp. 75–78, 2006.
[35] Y. L. Li, J. Millen and P. F. Barker, "Simultaneous cooling of coupled mechanical oscillators using whispering gallery mode resonances," *Opt. Express*, vol. 24, no. 2, pp. 1392–1401, 2016.
[36] S. Basiri-Esfahani, A. Armin, S. Forstner, and W. P. Bowen, "Precision ultrasound sensing on a chip," *Nat. Commun.*, vol. 10, no. 1, p. 132, 2019.
[37] M. A. Khalighi, and M. Uysal, "Survey on free space optical communication: a communication theory perspective," *IEEE Commun. Surveys Tuts.*, vol. 16, no. 4, pp.2231–2258, 2014.
[38] M. L. Gorodetsky, A. A. Savchenkov, and V. S. Ilchenko, "Ultimate Q of optical microsphere resonators," *Opt. Lett.*, vol. 21, no. 7, p. 453–455, 1996.
[39] R. Buchner, J. Barthel, and J. Stauber, "The dielectric relaxation of water between 0 °C and 35 °C," *Chem. Phys. Lett.*, vol. 306, no. 1–2, pp. 57–63, 1999.
[40] D. C. Dube, M. T. Lanagan, J. H. Kim, and S. J. Jang, "Dielectric measurements on substrate materials at microwave frequencies using a cavity perturbation technique," *J. Appl. Phys.*, vol. 63, no. 7, pp. 2466–2468, 1988.
[41] T. Carmon, L. Yang, and K. J. Vahala, "Dynamical thermal behavior and thermal self-stability of microcavities," *Opt. Express*, vol. 12, no. 20, pp. 4742–4750, 2004.
[42] D. Armani, B. Min, A. Martin, and K. J. Vahala, "Electrical thermo-optic tuning of ultrahigh-Q microtoroid resonators," *Appl. Phys. Lett.*, vol. 85, no. 22, pp. 5439–5441, 2004.
[43] Y. Feng, Y. Zheng, F. Zhang, J. Yang, T. Qin,and W. Wan, "Passive fine-tuning of microcavity whispering gallery mode for nonlinear optics by thermo-optical effect," *Appl. Phys. Lett.*, vol. 114, no. 10, p. 101103, 2019.
[44] Z. Zhou, C. Zou, Y. Chen, Z. Shen, G. Guo, and C. Dong, "Broadband tuning of the optical and mechanical modes in hollow bottle-like microresonators," *Opt. Express*, vol. 25, no. 4, pp. 4046–4053, 2017.
[45] K. Lai, H. Peng, W. Kundhikanjana, et al., "Nanoscale electronic inhomogeneity in In2Se3 nanoribbons revealed by microwave

impedance microscopy," *Nano. Lett.*, vol. 9, no. 3, pp. 1265–1269, 2009.
[46] E. Seabron, S. MacLaren, X. Xie, S. V. Rotkin, J. A. Rogers, and W. L. Wilson, "Scanning probe microwave reflectivity of aligned single-walled carbon nanotubes: imaging of electronic structure and quantum behavior at the nanoscale," *ACS Nano.*, vol. 10, no. 1, pp. 360–368, 2015.
[47] H. P. Huber, M. Moertelmaier, T. M. Wallis, et al., "Calibrated nanoscale capacitance measurements using a scanning microwave microscope," *Rev. Sci. Instrum.*, vol. 81, no. 11, p. 113701, 2010.
[48] O. D. Incel, "A survey on multi-channel communication in wireless sensor networks," *Comput. Netw.*, vol. 55, no. 13, pp. 3081–3099, 2011.
[49] I. F. Akyildiz, D. Pompili, and T. Melodia, "Underwater acoustic sensor networks: research challenges," *Ad. Hoc. Netw.*, vol. 3, no. 3, pp. 257–279, 2005.

Supplementary Material: The online version of this article offers supplementary material https://doi.org/10.1515/nanoph-2020-0176.